



**HAL**  
open science

## Cell surface protein-protein interaction analysis with combined time-resolved FRET and snap-tag technologies: application to GPCR oligomerization

Damien Maurel, Laetitia Comps-Agrar, Carsten Brock, Marie-Laure Rives, Emmanuel Bourrier, Mohammed Akli Ayoub, Hervé Bazin, Norbert Tinel, Thierry Durroux, Laurent Prézeau, et al.

### ► To cite this version:

Damien Maurel, Laetitia Comps-Agrar, Carsten Brock, Marie-Laure Rives, Emmanuel Bourrier, et al.. Cell surface protein-protein interaction analysis with combined time-resolved FRET and snap-tag technologies: application to GPCR oligomerization. *Nature Methods*, 2008, 5 (6), pp.561. 10.1038/nmeth.1213 . hal-00318856

**HAL Id: hal-00318856**

**<https://hal.science/hal-00318856>**

Submitted on 5 Sep 2008

**HAL** is a multi-disciplinary open access archive for the deposit and dissemination of scientific research documents, whether they are published or not. The documents may come from teaching and research institutions in France or abroad, or from public or private research centers.

L'archive ouverte pluridisciplinaire **HAL**, est destinée au dépôt et à la diffusion de documents scientifiques de niveau recherche, publiés ou non, émanant des établissements d'enseignement et de recherche français ou étrangers, des laboratoires publics ou privés.

**Cell surface protein-protein interaction analysis with combined time-resolved FRET and snap-tag technologies: application to GPCR oligomerization**

Damien Maurel<sup>1,2,3,4</sup>, Laetitia Comps-Agrar<sup>1,3</sup>, Carsten Brock<sup>1</sup>, Marie-Laure Rives<sup>1</sup>, Emmanuel Bourrier<sup>2</sup>, Mohammed Ayoub<sup>1</sup>, Hervé Bazin<sup>2</sup>, Norbert Tinel<sup>2</sup>, Thierry Durroux<sup>1</sup>, Laurent Prézeau<sup>1</sup>, Eric Trinquet<sup>2</sup> and Jean-Philippe Pin<sup>1</sup>

<sup>1</sup> CNRS,UMR 5203, Institut de Génomique fonctionnelle, Montpellier, France and INSERM,U661, Montpellier, France and Université Montpellier 1,2, Montpellier F-34000, France.

<sup>2</sup> CisBio International, Parc technologique Marcel Boiteux, Bagnols/Cèze cedex F-30204, France

<sup>3</sup>: these authors contributed equally to this work

<sup>4</sup> present address: Ecole Polytechnique Fédérale de Lausanne, Institute of Chemical Sciences and Engineering, CH-1015 Lausanne, Switzerland

**Correspondence should be addressed to J.P.P ([jppin@igf.cnrs.fr](mailto:jppin@igf.cnrs.fr))**

Institut de Génomique Fonctionnelle

141, rue de la cardonille

34094, Montpellier cedex 5, France

fax: +33 (0)4 67 64 24 32

## Abstract

Cell surface proteins play key roles in cell-cell communication. They assemble into hetero-complexes that include different receptors and effectors. Demonstrating and manipulating such protein complexes will certainly offer new ways for new therapeutics. Here we developed reagents to quantitatively analyze in a high throughput format protein-protein interaction at the surface of living cells. Using this approach we examined whether G-protein coupled receptors (GPCRs) are monomers or assemble into dimers or larger oligomers, a matter of intense debates. We bring new evidence for the oligomeric state of both class A and class C GPCRs. We also report a different quaternary structure of the GPCRs for the two major neurotransmitters. Whereas metabotropic glutamate receptors assemble into strict dimers, the GABA<sub>B</sub> receptor spontaneously form dimers of heterodimers offering a way to modulate G-protein coupling efficacy. This approach will be useful to systematically analyze the dynamics of cell surface protein complexes in living cells.

Cell-cell communication involves cell surface proteins such as receptors, cell adhesion molecules, channels and transporters. Among these proteins, the G-protein-coupled receptors (GPCRs) form the largest family of membrane signaling molecules and represent the major target for drug development<sup>1</sup>. Although these 7 transmembrane helix proteins can activate heterotrimeric G proteins in a monomeric form<sup>2-5</sup>, much interest arises from their possible assembly into larger complexes<sup>6,7</sup>. GPCRs may not only oligomerize, but also associate with other membrane proteins such as channels, enzymes, other receptor types and transporters. Such complexes are proposed to allow faster signaling, specific cross-talks, or specific responses. However, such organization of GPCRs remains a matter of intense debate<sup>3,8-10</sup>. Even if such oligomers exist, their stoichiometry - i.e. dimers versus higher-order oligomers - is not known.

Today resonance energy transfer (RET) technologies are widely used to validate the proximity between proteins in living cells<sup>11,12</sup>. These approaches are based on the fusion of FRET compatible GFP variants, or Luciferase and GFP for bioluminescence RET (BRET). However, the fusion proteins are often over-expressed in transfected cells such that FRET can occur within intracellular compartments where proteins accumulate, making difficult the demonstration that RET results from a direct interaction of the proteins at the cell surface. To overcome this problem, few studies took advantage of the use of antibodies carrying fluorophores to specifically label surface proteins<sup>13,14</sup>. Another limitation of the commonly used RET techniques is the low signal to noise ratio due to the overlap between the emission spectra of donors and acceptors, and intrinsic fluorescence of the cells. Time-resolved FRET (TR-FRET) approach based on the use of europium cryptate as donors, and alexafluor647 or d2 as acceptors, offers a much higher signal to noise ratio for two main reasons. First, the long life-time of the europium allows the measurement of FRET emission when all natural fluorophores are switched off<sup>15</sup> (supp Fig. Aa), and second, this donor fluorophore has a very limited emission at 665nm where the acceptor emission is measured<sup>15</sup> (supp Fig. Ab). Association of TR-FRET with antibodies has therefore been used to validate the existence of GPCR oligomers at the surface of living cells<sup>13,14,16</sup>. However, the bivalent nature of antibodies could well stabilize large complexes. Moreover, the size (150 kDa, 160Å in length) (Fig. 1a) and multiple labeling of these proteins can easily increase FRET resulting from random collision.

Here we used the newly developed snap-tag technology to specifically label surface proteins with TR-FRET compatible fluorophores<sup>17,18</sup>. Snap-tag derives from the O<sup>6</sup>-guanine nucleotide alkyltransferase that covalently reacts with benzyl-guanines (BG) (Fig 1b). This tag, two third

the size of GFP (Fig 1a), can be specifically and covalently labeled with any fluorophore carried by the benzyl-group of BG. By generating non-permeant BG derivatives compatible with TR-FRET measurement, we confirm here the oligomeric assembly of both class A and class C GPCRs. Using an optimized quality control system that allows the specific labeling of a single subunit in a dimer, we show moreover that the metabotropic glutamate (mGlu) receptors assemble into strict dimers, whereas the GABA<sub>B</sub> receptors can form dimers of dimers. This approach will be useful to rapidly and quantitatively analyze in a high throughput format other cell surface signaling complexes in living cells allowing the rapid identification of molecules, antibodies or other protein partners affecting these complexes.

## RESULTS

### **Labeling of surface receptors with TR-FRET compatible fluorophores**

Among the large GPCR family, receptors activated by GABA (the GABA<sub>B</sub> receptors) are composed of two distinct subunits, GABA<sub>B1</sub> where agonists bind and GABA<sub>B2</sub> that activates G-proteins<sup>19</sup> (Fig. 1a). Of note, GABA<sub>B1</sub> possesses an intracellular retention sequence in its C-terminal tail that prevents it from reaching the cell surface, unless associated with GABA<sub>B2</sub> through a coiled coil interaction of their C-terminal tails<sup>20,21</sup>. These receptors constitute therefore an excellent model to test new approaches to quantify protein-protein interactions at the cell surface.

A snap-tag was introduced at the N-terminal end of GABA<sub>B</sub> subunits. Both fusion proteins were correctly expressed and showed no alteration of their functional properties (supp Fig. B). We next prepared BG derivatives carrying either an europium cryptate (BG-K) (supp materials and supp Fig. C), or the acceptor d2 (BG-d2) on the benzyl group. A clear specific labeling can be detected with these BG derivatives when ST-GABA<sub>B1</sub> is at the cell surface after co-expression with GABA<sub>B2</sub>, or when its intracellular retention signal is mutated (Fig. 1c-e). In contrast, no specific labeling could be observed in cells expressing ST-GABA<sub>B1</sub> alone (Fig. 1d), unless cells are permeabilized. Similar data were obtained with the intracellular protein G $\alpha$ i fused to ST (Fig. 1d). Fluorescence imaging also confirmed that only the cell surface ST-proteins are labeled (Fig. 1e). Specific bound fluorescence was used to estimate the number of snap-tags labeled under these conditions. By comparing these values with the total amount of binding sites at the cell surface, we found that both BG derivatives label all surface receptors over a wide range of receptor expression (Fig. 1f).

### **Detection of cell surface GABA<sub>B</sub> heteromers with combined snap-tags and TR-FRET**

The ST-fusion versions of GABA<sub>B1</sub> and GABA<sub>B2</sub> when then used to examine whether ST could be used to detect protein-protein interaction at the cell surface. Large TR-FRET signals could be measured in cells expressing ST-GABA<sub>B1</sub> and flag-GABA<sub>B2</sub> after labeling with BG-K and anti-flag antibodies carrying the d2 acceptor (Fig. 2a). The same was obtained with the BG-d2 and an anti-flag labeled with the europium-cryptate, demonstrating that TR-FRET can be used to monitor protein-protein interactions with snap-tag fusion proteins. The simplicity of the approach allowed us to examine the possible interaction of the flag-tagged GABA<sub>B</sub> receptor with a number of other cell surface snap-tag fusions (Fig. 2b). In most cases, no significant TR-FRET signals were measured (Fig. 2b) despite a similar expression of all constructs, demonstrating the specificity of this assay (data not shown).

To avoid the use of antibodies, we also show that GABA<sub>B</sub> heteromers can be detected in cells expressing ST-GABA<sub>B1</sub> and ST-GABA<sub>B2</sub> after double labeling the cells with both BG-K and BG-d2. In that case, conditions were defined to make sure of the equivalent labeling of the snap-tags with either fluorophores. To that aim, a sub-optimal concentration of BG-K was used (5 $\mu$ M) with an increasing concentration of BG-d2, and the optimal ratio of both BG concentrations was determined as that giving rise to maximal TR-FRET (Fig. 2c). Of note, this signal measured as the specific emission at 665 nm, was directly proportional to the amount of receptors at the cell surface (Fig. 2d). Under these conditions, the TR-FRET efficacy can be defined as the ratio between the acceptor emission, and the amount of donor fluorophores linked to the receptor. Of interest, the TR-FRET efficacy is constant over a wide range of receptor density at the cell surface (Fig. 2e), demonstrating that this FRET signal does not result from random collision of the labeled proteins, but from their physical interaction.

### **Oligomeric state of other GPCRs and other cell surface proteins**

Although class C GPCRs are well recognized as stable dimers, the possible oligomeric state of class A GPCRs is still a matter of intense debate<sup>8,9</sup>. Using N-terminal snap-tag versions of several GPCRs including V2 and V1a vasopressin,  $\beta$ 2-adrenergic, A1 adenosine, thrombin receptor (protease activated receptor 1), as well as the class B GPCR for PACAP and CD4, a membrane receptor with a single TM also known to form dimers, we show here that large FRET signals can be measured, in the same range in terms of efficacy to that observed

between both subunits of the GABA<sub>B</sub> dimer (Fig. 3a,b). The 2-3 fold variations observed in the FRET efficacy depending on the receptor being studied is compatible with distance variations between the fluorophores due to the snap-tag fusion to the N-terminus of the receptors (see supp. Fig. F, for the relation between distances and FRET efficacy). However, we cannot exclude the possibility that for the receptors showing a lower FRET intensity, that only a fraction of the receptors are associated in homodimers. However, because of the linear relationship between the TR-FRET intensity and the amount of receptors at the cell surface (Fig. 3a and data not shown), the proportion of homodimers is likely constant over the range of expression level examined. These data further demonstrate that GPCR can form dimers at the cell surface that can be easily detected with this approach.

### **mGluR1 dimers do not form higher-order oligomers**

It is still not clear whether GPCR complexes are limited to dimers or whether higher order oligomers exist. Here we examined whether the well recognized mGlu receptor homodimers<sup>19</sup> can form higher ordered oligomers. To that end we used the optimized quality control system that we recently developed to control the subunit composition of a mGlu dimer<sup>22</sup>. This system is based on the use of the GABA<sub>B1</sub> intracellular tail (C1), and that of GABA<sub>B2</sub> in which the intracellular retention signal KKDL (C2) was inserted after the coiled-coil domain. Accordingly, none of the mGlu receptor subunit carrying either the C1 or the C2 tail reach the cell surface alone, but do so when both subunits are co-expressed in the same cells (supp Fig. D)<sup>22</sup>. Moreover, this system does not affect normal functioning of the mGlu dimer<sup>22</sup>. Using this system, we can ascertain that all mGlu dimers at the cell surface carry a single snap-tag therefore allowing us to detect any possible interaction between mGlu dimers (Fig. 3c). Surprisingly, no significant signal was observed (Fig. 3c). This is in contrast to the large signal obtained when both subunits are labeled. This shows that under these conditions mGluR1 complexes are limited to strict dimers. Of note, these data further confirm the specificity of the GPCR dimers described above since no FRET signal can be measured between mGlu dimers despite their large expression level at the cell surface (Fig. 3c).

### **GABA<sub>B</sub> heterodimers can form dimers of dimers**

Using the snap-tag approach and the optimized quality control system, we also analyzed the oligomeric assembly of the GABA<sub>B</sub> receptor. In contrast to what was observed with the mGlu1 receptor, a large TR-FRET signal was obtained in cells expressing GABA<sub>B</sub> receptors labeled on their GABA<sub>B1</sub> subunit only (Fig. 4a), a signal close to that measured between

GABA<sub>B1</sub> and GABA<sub>B2</sub>. Again, the TR-FRET efficacy is constant over a wide range of GABA<sub>B</sub> receptor expression including at the physiological density of 0.5 pmol of receptors per mg protein<sup>23</sup>. Similar data were obtained with both GABA<sub>B1</sub> splice variants, GABA<sub>B1a</sub> and GABA<sub>B1b</sub> that differ by the presence of a pair of sushi domains at their N-terminus<sup>24</sup> (supp Fig. E).

Surprisingly, very low TR-FRET signal was observed when only the GABA<sub>B2</sub> subunits are labeled (Fig. 4a). This low signal does not result from a peculiar association of these subunits leading to an absence of energy transfer. First, due to the encaging of Europium, the donor dipole is not constraint, such that the low FRET cannot be due to an incompatible dipole-dipole orientation<sup>25</sup>. Second, when expressed alone, GABA<sub>B2</sub> subunits form homodimers that can be detected using ST-GABA<sub>B2</sub> (Fig. 4b). This signal is largely inhibited by increasing the amount of GABA<sub>B1</sub> (Fig. 4c), consistent with GABA<sub>B1</sub> competing with GABA<sub>B2</sub> in GABA<sub>B2</sub> homodimers.

These results revealed a close proximity of the GABA<sub>B1</sub> subunits, but not between GABA<sub>B2</sub>. This is not consistent with a random clustering or an accumulation of GABA<sub>B</sub> heterodimers into microdomains, or to a dissociation-reassociation of the subunits at the cell surface since in those cases similar FRET should be observed between GABA<sub>B2</sub> and between GABA<sub>B1</sub> subunits. This is more consistent with a specific organization of the GABA<sub>B</sub> heteromers into at least dimers of dimers, interacting via the GABA<sub>B1</sub> subunit. This model is compatible with the FRET efficacies measured between the different subunits. Indeed, the  $R_0$  for the FRET pair used is 65Å, giving rise to a FRET efficacy of more than 90% according to the Förster's equation for fluorophores distant of 35Å corresponding to the distance between the N-termini of the two subunits (supp Fig. F). In contrast, a FRET efficacy lower than 20% can be calculated for fluorophores distant of more than 80Å, a distance between GABA<sub>B2</sub> subunits compatible with GABA<sub>B</sub> dimers interacting via their GABA<sub>B1</sub> subunits only (supp Fig. F).

Such a general quaternary structure and organization of the GABA<sub>B</sub> oligomer is not influenced by receptor activation since GABA stimulation did not change the TR-FRET signal measured between any subunits of the oligomer (Fig. 4d).

### **Functional correlate of the dimerization of GABA<sub>B</sub> heterodimers.**

To examine if the quaternary organization of the GABA<sub>B</sub> receptor could be correlated with specific functional properties, we prevented the association between GABA<sub>B</sub> dimers using a minimal domain of GABA<sub>B1</sub> corresponding to the heptahelical domain (GB1-HD) (Fig. 5a). Of note, this domain is known not to activate G-proteins<sup>19</sup>. This GB1-HD was found to

compete with the full length GABA<sub>B1</sub> in the dimer-dimer interaction, as illustrated by the total inhibition of the TR-FRET between ST-GABA<sub>B1</sub> subunits (Fig. 5a (1)). In parallel, an increase in the TR-FRET signal between ST-GABA<sub>B1</sub> and HA-GB1-HD was observed, demonstrating that GB1-HD interacts with the full length GABA<sub>B1</sub> subunit (Fig. 5a (2)). However, no inhibition of the FRET between GABA<sub>B1</sub> and GABA<sub>B2</sub> was observed (Fig. 5a (3)). It is important to point out that this experiment was conducted using a GABA<sub>B2</sub> subunit carrying an ER retention signal, such that any possible heterodimer between GB1-HD and GABA<sub>B2</sub> are retained inside the cells since the GB1-HD lacks the C-tail required to mask the retention signal (Fig. 5a, and supp Fig. G). The absence of clear competition between full-length GABA<sub>B1</sub> and GB1-HD for interaction with GABA<sub>B2</sub> was expected because the GABA<sub>B</sub> heterodimer is strongly stabilized by i) the coiled-coil interaction of the C-terminal tails and ii) the direct interaction of the large extracellular domains<sup>19</sup>, two contacts being absent in a GABA<sub>B2</sub>-GB1-HD dimer.

Under these conditions, when most dimers of GABA<sub>B</sub> heterodimers were dissociated (Fig. 5b), and even though the same amount of the G protein-activating subunit GABA<sub>B2</sub> were found at the cell surface (data not shown), maximal agonist-mediated response was twice that measured under control condition (Fig. 5b). No such effect was observed after over-expression of CD4 that did not inhibit the association between GABA<sub>B</sub> dimers (Fig. 5b and data not shown). This brings a functional correlate to the quaternary structure of this GABA receptor and suggests that the association of GABA<sub>B</sub> dimers into dimers of dimers offers a way to modulate G-protein coupling efficacy.

## DISCUSSION

Here, we presented a new approach to analyze protein-protein interaction at the cell surface based on a combination of TR-FRET and snap-tag technologies. We validated this approach using well recognized GPCR dimers, the GABA<sub>B</sub> and mGlu1 receptors, and confirm that both class A and B receptors also form dimers or larger oligomers at the cell surface. When associated with a quality control system allowing the labeling of a single subunit, we show that whereas only strict dimers of mGluR1 could be observed, the GABA<sub>B</sub> receptor assembles into at least dimers of dimers.

Although FRET and BRET have been widely used to analyze the oligomeric state of membrane proteins, the low signal to noise ratio made difficult the use of such techniques in screening assays. Moreover, it was still difficult to prove that the signals obtained originate from the cell surface. Indeed, even though a nice and saturable BRET signal could be

measured between GABA<sub>B1</sub> in the presence of GABA<sub>B2</sub> (supp Fig. H), we could not exclude that this signal originate from intracellular GABA<sub>B1</sub> homodimers<sup>26</sup>. Although, imaging techniques and total internal reflection fluorescence microscopy can be used to examine FRET at the plasma membrane, such approaches are not compatible with systematic and quantitative assessments of the interaction. In contrast, the TR-FRET snap-tag technology, by allowing an easy assessment of the protein proximity at the cell surface enables a clear demonstration of the specificity of the interaction. Indeed, the assay was conducted in 96 well plates, and can easily be adapted to 384 plates as many other TR-FRET cellular assays. Of note, a very low emission of the acceptor is observed when non-interacting proteins are being studied, showing that even with over-expressed proteins, very low FRET occurs due to random collision at the cell surface. This suggests that the high non-specific "by stander" FRET or BRET measured with GFP or Rluc fused membrane proteins likely originate from the intracellular proteins.

Within the last 10 years, a large number of studies reported that GPCRs can form oligomers, but it was still not known whether such complexes were limited to dimers or whether higher-order oligomers could form<sup>6,7,27</sup>. By taking advantage of an optimized quality control system, we show here that mGlu1 dimers cannot on their own self associate, demonstrating that a dimeric organization of these receptors is sufficient for function. One of course cannot exclude the possibility that, in their native environment, these mGlu dimers can associate into larger complexes through interaction with scaffolding proteins. To our surprise however, we found that the GABA<sub>B</sub> receptor heterodimer can form larger oligomers through GABA<sub>B1</sub> interaction. Because no close proximity between GABA<sub>B2</sub> subunits was observed, it is likely that these oligomers are limited to dimers of dimers. Accordingly, as for any other GPCR homodimer such a quaternary organization of the GABA<sub>B</sub> receptor possesses two agonists binding sites, and two possible G-protein coupling domains. Importantly, this organization of the GABA<sub>B</sub> receptor can be observed over a wide range of receptor density at the cell surface, including that reported for this receptor in the brain<sup>23</sup>. Since the receptor density is expected to be even higher in the specific micro domains where this receptor is targeted in neurons (dendritic spines and pre-synaptic terminals), this makes likely that what is observed here in transfected cells can also occur *in vivo*, unless specific interacting proteins absent in HEK or COS cells prevent this.

By preventing GABA<sub>B</sub> heterodimers to associate, using a minimal domain of GABA<sub>B1</sub>, we also provide a functional evidence in favor of the dimer of dimer organization of the GABA<sub>B</sub> receptor. Our data are consistent with a lower G protein-coupling efficacy of the GABA<sub>B</sub>

receptor when associated into dimers of dimers. Of interest, such a dimerization of the GABA<sub>B</sub> heterodimer reproduces what has been recently shown for GPCR homodimers. Indeed, in GPCR homodimers, a single subunit can activate a G-protein at a time<sup>2,28-30</sup>. Since GPCR monomers can effectively activate G-proteins<sup>2-5</sup>, then two separated monomers are expected to activate more G-proteins than a homodimer. This has been recently demonstrated for both rhodopsin<sup>2</sup> and the neurotensin1 receptor<sup>30</sup>. Such a process could be a way to modulate coupling efficacy *in vivo*, or to allow simultaneous coupling to both G protein-dependent and G protein-independent pathways, but more work is required to validate this proposal.

In conclusion, we showed here that the combined use of snap-tag and TR-FRET allows a rapid, easy and quantitative assessment of cell surface protein interactions. This approach confirmed the oligomeric assembly of GPCRs at the cell surface and allowed us to analyze the stoichiometry of class C GPCR oligomers. This technology will certainly be useful to study the dynamics of any cell surface protein complexes, and to identify drugs that modulate these.

## **Methods**

### **Plasmids and site-directed mutagenesis**

Plasmids encoding the wild-type GABA<sub>B1</sub>, GABA<sub>B2</sub> and mGlu1 subunits epitope-tagged at their N-terminus with HA and Flag after the signal peptide of the mGlu5 receptor were described previously<sup>16</sup>. SNAP-tag sequence (obtained from the pSST26m plasmid from Covalys, Geneva, Switzerland) was subcloned in these plasmids at the level a unique MluI restriction site located in the linker downstream of the HA or flag tag. The upstream Mlu-I site was then mutated to conserve a unique Mlu-I site between the SNAP-tag and the GABA<sub>B</sub> coding sequence. These plasmids were then used to introduce the coding sequence of various membrane proteins in phase with the snap-tag, these include the coding sequences of mGlu1, V2 and V1a vasopressin, β2-adrenergic, A1 adenosine, PACAP, protease-activating 1 (thrombin receptor), and prolactin receptors and that of CD4. The HA-GB1-HD truncated construct was made after insertion of a second Mlu-I site at the level of codons for residues 573-574 in the HA-GABA<sub>B1</sub> sequence. The fragment between the two Mlu-I sites was then removed, and a stop codon was introduced at position 875 using a Quick-Change® strategy (Stratagene).

### **Cell culture and transfection**

HEK-293 or COS-7 cells were cultured in Dulbecco's modified Eagle's medium supplemented with 10% FCS and transfected by electroporation as described previously<sup>14</sup>. Culture medium, FCS, and other products used for cell culture were purchased from GIBCO/BRL/Life Technologies (Cergy Pontoise, France). Ten million cells were transfected with plasmid DNA expressing the proteins of interest as indicated in the figures and completed to a total amount of 10  $\mu$ g plasmid DNA with pRK5 empty vector.

### **ELISA assay for quantification of cell surface expression**

Cells were fixed with 4% paraformaldehyde and then blocked with phosphate-buffered saline + 1% fetal calf serum. After a 30 min incubation, the anti-HA monoclonal antibody (clone 3F10, Roche Bioscience, Basel, Switzerland) or anti-Flag-M2 monoclonal antibody (Sigma-Aldrich, St. Louis, MO, USA), both conjugated with horseradish peroxidase, was applied for 30 min at 0.5 mg/l and cells were washed. Bound antibody was detected by chemoluminescence using SuperSignal substrate (Pierce, Rockford, IL, USA) and a Wallac Victor<sup>2</sup> counter (Molecular Devices, Sunnyvale, CA, USA). Validation of this assay has already been reported<sup>16,29</sup>.

### **Intracellular calcium measurements**

Twenty-four hours after transfection with plasmids encoding the indicated GABA<sub>B</sub> subunits and a chimeric protein Gqi9, HEK-293 cells were washed with HBSS buffer (20 mM HEPES, 1 mM MgSO<sub>4</sub>, 3,3 mM Na<sub>2</sub>CO<sub>3</sub>, 1,3 mM CaCl<sub>2</sub>, 0,1% BSA, 2,5 mM probenecid) and loaded with 1  $\mu$ M Ca<sup>2+</sup>-sensitive fluorescent dye Fluo-4 a.m. (Molecular Probes, Eugene, OR, USA) for 1 h at 37°C. After a wash, cells were incubated with 50  $\mu$ l of buffer and 50  $\mu$ l of 2X-GABA solution at various concentrations was added after 20 s of recording. Fluorescence signals (excitation 485 nm, emission 525 nm) were measured by using the fluorescence microplate reader Flexstation (Molecular Devices, Sunnyvale, CA, USA) at sampling intervals of 1.5 s for 60 s. Data were analyzed with the program Soft Max Pro (Molecular Devices, Sunnyvale, CA, USA). Dose-response curves were fitted using Prism (GraphPad software, San Diego, CA, USA).

### **Confocal imaging**

HEK-293 cells were transfected with the indicated plasmids as described above. Snap-tag labeling was performed with 1  $\mu$ M BG-d2. Coverslips were mounted with Gel / Mount (Biomedex, Foster City, CA). Confocal imaging was performed with a Plan-Apochromat 63 x / 1.4 oil objective and Immersol 518F (Carl Zeiss, Jena, Germany). GFP was excited at 488 nm and detected through a 505 - 530 nm band pass filter. d2 was excited at 633 nm and detected through a 650 nm long pass filter. Pinholes were adjusted to yield optical slices of < 0.5 nm.

### **Binding assay**

Cells were incubated with increasing concentrations of radioactive tracer (0.48 nM to 10 nM of [<sup>3</sup>H]-CGP54626, a radioactive antagonist of GABA<sub>B</sub> receptor) for 4 hours at 4°C. For each concentrations of tracer, non specific binding was determined by addition of GABA (1mM). After incubation, cells were washed with Tris-KREBS buffer (20 mM Tris pH 7.4, 118 mM NaCl, 5.6 mM glucose, 1.2 mM KH<sub>2</sub>PO<sub>4</sub>, 1.2 mM MgSO<sub>4</sub>, 4,7 mM KCl, 1.8 mM CaCl<sub>2</sub>) in order to eliminate the excess of free radioactive ligand. Cells were then lysed using NaOH at 0.1 M for 10 min and transferred in flasks containing scintillant (OptiPhase Supermix, Perkin Elmer). Radioactivity was counted on a Beta counter Cobra (Hewlett Packard). Fitting parameters for saturation experiments were determined using a non-linear curve-fitting routine to the Hill equation  $B = B_{max} [L] / ([L] + K_d)$  where B<sub>max</sub> is the maximal binding, L is the concentration of labeled ligand and K<sub>d</sub> the equilibrium dissociation constant for the labeled ligand.

### **BG-K synthesis**

The O<sup>6</sup>-(4-Aminomethyl-benzyl)guanine **1** (0.6 mg, 2.2  $\mu$ mol) (supp Fig. C) was dissolved in 450  $\mu$ l of 100 mM phosphate buffer pH7 and 50  $\mu$ l of dimethylformamide, 4.3  $\mu$ mol of SMCC (Succinimidyl-4-[N-maleimidomethyl]cyclohexane-1-carboxylate) dissolved in 220  $\mu$ l of acetonitrile were added. After 90 min reaction at room temperature the HPLC (Chromolith gradient A detection 280 nm) showed consumption of the starting guanine derivative ( $t_r$  = 6.2 min) apparition of a new peak ( $t_r$  = 18.2 min) and some residual SMCC ( $t_r$  = 19.6 min). The reaction mixture was acidified with 300  $\mu$ l of 1% aqueous TFA and the purified by HPLC using the above conditions, the fraction containing the maleimide derivative **2** were evaporated to dryness and co-evaporated with water (vacuum-centrifuge), then dissolved in acetonitrile / water mixture (2:8, v/v) for UV quantitation ( $\epsilon_{285} \text{ nm} = 12\,000 \text{ M}^{-1} \cdot \text{cm}^{-1}$ ). Yield

0.77  $\mu\text{mol}$ . ES+:  $(\text{M}+\text{H})^+ = 490.3$  ,  $(\text{M}+\text{Na})^+ = 490.3$  , ES-:  $(\text{M}-\text{H})^- = 488.4$ .

The Eu $\zeta$ PBBP-NH<sub>2</sub> cryptate **3** [US Patent 7,087,384] (5.5 mg , 4 mmol) in 1.8 ml of 100mM phosphate buffer pH 7 ( $t_{\text{R}} = 9.4$  min , gradient B), was treated with SPDP (N- succinimidyl 3-(2-pyridyldithio) propionate) (8  $\mu\text{mol}$ ) and after 90 mn TCEP (Tris(2-carboxyethyl)phosphine hydrochloride) (9  $\mu\text{mol}$ ) was added. After 10 min the reduction was complete and the thiolated cryptate **4** ( $t_{\text{R}} = 8.3$  min) was purified over HPLC, the relevant fractions were evaporated to dryness. Compound **4** (3  $\mu\text{mol}$ ) was dissolved in 1.6 ml of 100 mM HEPES buffer pH 6.5 and the maleimido-benzylguanine **2** (in 0.2 ml of HEPES and 0.2 ml ACN) was added. After 30 mn HPLC analysis (gradient B) showed the formation of a new peak ( $t_{\text{R}} = 12.8$  min), the reaction mixture was acidified with 1% TFA and immediately purified using the same gradient conditions. The title compound **5** (BG-K) was collected and the fractions were evaporated to dryness, co-evaporated with water to remove any residual TFA, and the residue dissolved in ACN / 20 mM TEAB (Triethylammonium hydrogen carbonate) (1:1 , v/v) quantified by UV absorbance ( $\epsilon_{320} = 24,000 \text{ M}^{-1}.\text{cm}^{-1}$ ) and stored as 100 nmol aliquots evaporated to dryness (vacuum-centrifuge) in eppendorf tubes. Yield 1.1  $\mu\text{mol}$  based on the maleimido-benzylguanine. ES+ :  $(\text{M}-2\text{H})^+ = 1487.5$  ,  $(\text{M}-2\text{H}+\text{TFA})^+ = 1601.6$  ,  $(\text{M}-2\text{H}+2\text{TFA})^+ = 1715.6$ . Calc. for C<sub>66</sub>H<sub>64</sub>EuN<sub>16</sub>O<sub>14</sub>S = 1489.37.

### **SNAP-tag labeling with TR-FRET compatible fluorophores**

Twenty four hours after transfection, cells (100 000 cells per well of a 96 Greiner CellStar well plate) were washed with DMEM 10% FCS pre-warmed at 37°C. Then, cells were labeled one hour at 37°C, 5% CO<sub>2</sub> with different concentrations of derivatized benzyl guanine (BG-K or BG-d2) in DMEM 10% FCS. After labeling, cells were washed four times with Tris-KREBS buffer (20 mM Tris pH 7.4, 118 mM NaCl, 5.6 mM glucose, 1.2 mM KH<sub>2</sub>PO<sub>4</sub>, 1.2 mM MgSO<sub>4</sub>, 4,7 mM KCl, 1.8 mM CaCl<sub>2</sub>) and the signal recorded under 100 $\mu\text{L}$  of Tris-Krebs per well. The emission signal from the cryptate was recorded at 620nm on a time-resolved fluorimeter (RubyStar, BMG Labtechnologies, Champigny-sur-Marne, France) after an excitation at 337nm by a nitrogen laser and the emission signal from the d2 was recorded at 682nm on an Analyst reader (Molecular Devices) using a 640nm excitation. Finally, the specific fluorescence signal was determined by subtracting the total fluorescence signal from the cells expressing the cell surface SNAP-tag protein with the non specific signal from mock transfected cells.

### **TR-FRET between SNAP-tag and antibodies labeled with the indicated fluorophores**

After SNAP-tag labeling with BG-K (see above), cells (100 000 cells per well of a 96 Greiner CellStar well plate) were incubated in Tris-Krebs with 2nM of anti-flag antibodies conjugated with d2 (means of 3.5 fluorophores per anti-flag M2 antibody), overnight at 4°C. Finally, the FRET signal was measured at 665nm between 50 and 450 $\mu$ s after laser excitation at 337 nm, without washing out the unbound antibodies (homogeneous format). Assay signals were expressed by the  $\Delta 665 = (\text{total signal recorded at 665nm}) - (\text{background at 665nm})$ . The background signal corresponds to SNAP-tag cells labeled with BG-K only (without antibodies). Similar background values were obtained with 2nM anti-flag-d2 and an excess of unlabeled anti-flag antibodies (1 $\mu$ M). Similar experiments were conducted with 2nM anti-HA conjugated with d2. A similar protocol was used to measure TR-FRET with BG-d2 labeling and europium cryptate-conjugated anti-flag or anti-HA antibodies. In those cases, the negatives correspond to the europium cryptate-conjugated anti-flag or anti-HA antibodies alone.

### **TR-FRET between two SNAP-tags**

Twenty four hours after transfection, cells were washed one time with 100 $\mu$ L of complete DMEM medium and then incubated one hour at 37°C, 5% CO<sub>2</sub> with a mixture of BG-K and BG-d2. The optimal concentration ratio was obtained for 5 $\mu$ M of BG-K with 0.5 $\mu$ M of BG-d2. After the labeling cells were washed four times with Tris-Krebs and the signal recorded on a Rubystar plate reader. Here, the  $\Delta 665$  represents the FRET signal recorded on BG-K/BG-d2 labeled cells from which the signal recorded on the same cells labeled with BG-K and a cold BG diluted at the same concentration than the BG-d2 was substrated.

### **Acknowledgements:**

The authors wish to thank Mrs C. Vol (IGF, Montpellier) for her expert assistance for the GPCR functional assays, Mr. F. Maurin (CBI, Bagnols/Cèze) for his participation in the synthesis of BG derivatives. The authors would like to express their special thanks to Prof Kai Johnsson (EPFL, Lausanne, Switzerland) for his support to this project, his critical reading of the manuscript and for providing us with snap-tag tools. The authors also thank Drs. P. Rondard (IGF, Montpellier, France) and Ralf Jockers (Institut Cochin, Paris, France) for their comments on the manuscript. Confocal Imaging was performed at the *Centre de Ressources*

*en Imagerie Cellulaire*, Montpellier, with the help of N. Lautredou. This work was made possible thanks to the screening facilities of the Institut Fédératif de Recherche n°3 (IFR3).

This work was supported by the Centre National de la Recherche Scientifique (CNRS), the Institut National de la Santé et de la Recherche Médicale (INSERM), CisBio International, and by grants from the French Ministry of Research, Action Concertée Incitative "Biologie Cellulaire Moléculaire et Structurale" (ACI-BCMS 328), the Agence Nationale de la Recherche (ANR-05-PRIB-02502, ANR-BLAN06-3\_135092 and ANR-05-NEUR-035), and by an unrestricted grant from Senomyx (La Jolla, CA, USA).

**Authors contributions:**

**DM** and **LCA** executed most of the experiments and participated in the writing of the manuscript, **CB** developed the system to control subunit composition, and performed the confocal experiments, **MLR** performed the experiments with mGlu1 receptor and the initial experiments with class A receptors, **EB** and **HB** synthesized the BG derivatives, **MA** participated in the BRET experiments, **NT** and **ET** supervised the work at CisBio, **TD** and **LP** supervised some aspects of the work at the IGF, **JPP** supervised the project and wrote the manuscript.

## References

1. Bockaert, J. & Pin, J.P. Molecular tinkering of G protein-coupled receptors: an evolutionary success. *Embo J* **18**, 1723-1729 (1999).
2. Bayburt, T.H., Leitz, A.J., Xie, G., Oprian, D.D. & Sligar, S.G. Transducin activation by nanoscale lipid bilayers containing one and two rhodopsins. *J Biol Chem* **282**, 14875-14881 (2007).
3. Chabre, M. & le Maire, M. Monomeric G-protein-coupled receptor as a functional unit. *Biochemistry* **44**, 9395-9403 (2005).
4. Ernst, O.P., Gramse, V., Kolbe, M., Hofmann, K.P. & Heck, M. Monomeric G protein-coupled receptor rhodopsin in solution activates its G protein transducin at the diffusion limit. *Proc Natl Acad Sci U S A* **104**, 10859-10864 (2007).
5. Whorton, M.R. et al. A monomeric G protein-coupled receptor isolated in a high-density lipoprotein particle efficiently activates its G protein. *Proc Natl Acad Sci U S A* **104**, 7682-7687 (2007).
6. Bouvier, M. Oligomerization of G-protein-coupled transmitter receptors. *Nat. Rev. Neurosci.* **2**, 274-286 (2001).
7. Milligan, G. G-protein-coupled receptor heterodimers: pharmacology, function and relevance to drug discovery. *Drug Discov Today* **11**, 541-549 (2006).
8. Bouvier, M., Heveker, N., Jockers, R., Marullo, S. & Milligan, G. BRET analysis of GPCR oligomerization: newer does not mean better. *Nat Methods* **4**, 3-4; author reply 4 (2007).
9. James, J.R., Oliveira, M.I., Carmo, A.M., Iaboni, A. & Davis, S.J. A rigorous experimental framework for detecting protein oligomerization using bioluminescence resonance energy transfer. *Nat Methods* **3**, 1001-1006 (2006).
10. Meyer, B.H. et al. FRET imaging reveals that functional neurokinin-1 receptors are monomeric and reside in membrane microdomains of live cells. *Proc Natl Acad Sci U S A* **103**, 2138-2143 (2006).
11. Pflieger, K.D. & Eidne, K.A. Illuminating insights into protein-protein interactions using bioluminescence resonance energy transfer (BRET). *Nat Methods* **3**, 165-174 (2006).
12. Selvin, P.R. The renaissance of fluorescence resonance energy transfer. *Nat Struct Biol* **7**, 730-734 (2000).
13. McVey, M. et al. Monitoring receptor oligomerization using time-resolved fluorescence resonance energy transfer and bioluminescence resonance energy transfer. The human delta -opioid receptor displays constitutive oligomerization at the cell surface, which is not regulated by receptor occupancy. *J Biol Chem* **276**, 14092-14099 (2001).
14. Maurel, D. et al. Cell surface detection of membrane protein interaction with homogeneous time-resolved fluorescence resonance energy transfer technology. *Anal Biochem* **329**, 253-262 (2004).
15. Bazin, H., Trinquet, E. & Mathis, G. Time resolved amplification of cryptate emission: a versatile technology to trace biomolecular interactions. *J Biotechnol* **82**, 233-250 (2002).
16. Kniazeff, J. et al. Closed state of both binding domains of homodimeric mGlu receptors is required for full activity. *Nat. Str. Mol. Biol.* **11**, 706-713 (2004).
17. Keppler, A., Pick, H., Arrivoli, C., Vogel, H. & Johnsson, K. Labeling of fusion proteins with synthetic fluorophores in live cells. *Proc Natl Acad Sci U S A* **101**, 9955-9959 (2004).

18. Keppeler, A. et al. A general method for the covalent labeling of fusion proteins with small molecules in vivo. *Nat Biotechnol* **21**, 86-89 (2003).
19. Pin, J.-P. et al. Allosteric functioning of dimeric Class C G-protein coupled receptors. *FEBS J* **272**, 2947-2955 (2005).
20. Brock, C., Boudier, L., Maurel, D., Blahos, J. & Pin, J.P. Assembly-dependent surface targeting of the heterodimeric GABAB Receptor is controlled by COPI but not 14-3-3. *Mol Biol Cell* **16**, 5572-5578 (2005).
21. Margeta-Mitrovic, M., Jan, Y.N. & Jan, L.Y. A trafficking checkpoint controls GABA(B) receptor heterodimerization. *Neuron* **27**, 97-106 (2000).
22. Brock, C. et al. Activation of a Dimeric Metabotropic Glutamate Receptor by Inter-Subunit Rearrangement. *J Biol Chem* **282**, 33000-33008 (2007).
23. Bischoff, S. et al. Spatial distribution of GABA(B)R1 receptor mRNA and binding sites in the rat brain. *J Comp Neurol* **412**, 1-16 (1999).
24. Kaupmann, K. et al. Expression cloning of GABA(B) receptors uncovers similarity to metabotropic glutamate receptors. *Nature* **386**, 239-246 (1997).
25. Selvin, P.R. & Hearst, J.E. Luminescence energy transfer using a terbium chelate: improvements on fluorescence energy transfer. *Proc Natl Acad Sci U S A* **91**, 10024-10028 (1994).
26. Villemure, J.F. et al. Subcellular distribution of GABA(B) receptor homo- and heterodimers. *Biochem J* **388**, 47-55 (2005).
27. Lopez-Gimenez, J.F., Canals, M., Pediani, J.D. & Milligan, G. The alpha1b-adrenoceptor exists as a higher-order oligomer: effective oligomerization is required for receptor maturation, surface delivery, and function. *Mol Pharmacol* **71**, 1015-1029 (2007).
28. Damian, M., Martin, A., Mesnier, D., Pin, J.P. & Banères, J.L. Asymmetric conformational changes in a GPCR dimer controlled by G-proteins. *EMBO J* **25**, 5693-5702 (2006).
29. Hlavackova, V. et al. Evidence for a single heptahelical domain being turned on upon activation of a dimeric GPCR. *EMBO J* **24**, 499-509 (2005).
30. White, J.F. et al. Dimerization of the class A G protein-coupled neurotensin receptor NTS1 alters G protein interaction. *Proc Natl Acad Sci U S A* **104**, 12199-12204 (2007).

## Figure legends:

**Figure 1.** The use of snap-tag to label surface proteins with TR-FRET compatible fluorophores. **(a)** Ribbon representations at the same scale of the heterodimeric GABA<sub>B</sub> receptor (left, as based on the structure of the dimer of mGlu1 extracellular domains (pdb accession number:1EWK), and the structure of a possible rhodopsin dimer (pdb: 1N3M)), an IgG (center, pdb: 1IGT) and a snap-tag (right, pdb 1EH6). **(b)** Covalent labeling of snap-tag fusion protein using O<sup>6</sup>-benzyl guanine derivatives carrying a fluorophore (F). **(c)** Cell surface specific binding with increasing concentrations of BG-K (filled circles) or BG-d2 (open circles) on ST-GABA<sub>B1</sub> co-expressed with GABA<sub>B2</sub>. **(d)** Specific BG-K labeling of mock transfected cells, and cells expressing the ST-GABA<sub>B1</sub> alone (ST-GB1) or co-expressed with GABA<sub>B2</sub> (ST-GB1:GB2), ST-GABA<sub>B1</sub> mutated in its intracellular retention motif (ST-GB1<sub>ASA</sub>), and the G-protein  $\alpha 1$  subunit fused to snap-tag (Gi1-ST). **(e)** Confocal imaging of cells over-expressing a ST-GABA<sub>B1</sub>-GFP fusion alone (right) or together with GABA<sub>B2</sub> (left) and labeled with BG-d2. **(f)** Amount of d2 (open circles) and K (closed circles) fluorophores specifically bound to cells expressing various amounts of ST-GABA<sub>B</sub> receptors at the cell surface. Cells were transfected with a fixed amount of ST-GABA<sub>B1</sub> and increasing amounts of GABA<sub>B2</sub> plasmids. The specific number of cell surface receptors (Bmax) was determined by Scatchard analysis using [<sup>3</sup>H]-CGP54626, a non permeant GABA<sub>B1</sub> specific antagonist. Linear regression revealed a slope (number of fluorophores per GABA<sub>B</sub> dimers) of 1.05 and 1.04 for the BG-K and BG-d2 labeling, respectively. Data in **c**, **d** and **f** are means  $\pm$  sem of triplicate determinations from a representative experiment.

**Figure 2.** Detection of GABA<sub>B</sub> heteromers at the cell surface using snap-tag and TR-FRET. **(a)** FRET intensity between d2-labeled anti-flag antibodies and BG-K labeled snap-tags in cells expressing increasing amounts of surface ST-GABA<sub>B1</sub> and flag-GABA<sub>B2</sub> receptors. FRET is measured as the specific d2 emission at 665nm after excitation of europium cryptate at 337 nm, the background signal measured in the absence of d2-antibodies being subtracted. The FRET intensity is represented according to the total number of receptors expressed at the cell surface. **(b)** TR-FRET was measured between flag-GABA<sub>B</sub> receptors labeled with d2-antibodies, and the indicated HA-snap-tag fusion proteins labeled with BG-K. Data were obtained with the same amount of snap-tag proteins at the cell surface as measured with anti-anti-HA ELISA, and a constant amount of flag-GABA<sub>B</sub> receptors. Positive control (left column) was performed with cells expressing ST-GABA<sub>B1</sub> and flag-GABA<sub>B2</sub>. **(c)** FRET

intensity was measured in cells expressing ST-GABA<sub>B1</sub> and ST-GABA<sub>B2</sub> with varying concentration of BG-d2 and 5 $\mu$ M BG-K. **(d)** FRET intensity is directly proportional to the amount of ST-GABA subunits at the cell surface. The number of snap-tags was deduced from the Bmax of [<sup>3</sup>H]-CGP54626. **(e)** FRET efficacy as determined by the ratio of the specific d2 emission at 665 nm resulting from FRET, and the fluorescence intensity (at 620 nm) of the specifically bound BG-K, is plotted as a function of the amount of snap-tags at the cell surface deduced from the Bmax of [<sup>3</sup>H]-CGP54626. Data in **(a)** and **(b)** are means  $\pm$  sem of triplicate determinations from a typical experiments. Data in **(d)** and **(e)** are triplicate determinations from 4 independent experiments.

**Figure 3.** Detection of cell surface protein oligomers using snap-tag fusions and TR-FRET. **(a)** Both TR-FRET intensity and HA-ELISA were measured for various expression levels of either GABA<sub>B</sub> (filled squares) or V2 vasopressin (open squares) HA-ST-fusions. **(b)** Experiments were conducted as in **(a)** for various other cell surface proteins, and means TR-FRET intensity over the ELISA signal (representing the slope) are presented. Negative control (right column "mGlu1 dimer") was performed using a mGlu1 receptor dimer carrying a single ST (see **(c)**). **(c)** FRET intensity was plotted as a function of the amount of mGlu1 receptor at the cell surface, when both subunits are fused to snap-tag (filled symbols) or when only one subunit per dimer is labeled (open symbols). To control the subunit composition of the mGlu1 receptor dimer, each subunit carries the C-terminal tail of either GABA<sub>B1</sub> (C1 in blue) with its natural intracellular retention signal (blue ball) or GABA<sub>B2</sub> (C2 in red) in which an intracellular retention signal was added (red ball). Coiled-coil interaction between C1 and C2 prevents intracellular retention of both proteins such that neither subunit reach the surface alone, but do so when co-expressed together (supp Fig. D).

**Figure 4.** Detection of GABA<sub>B</sub> dimers of dimers at the cell surface. **(a)** FRET intensity (left panel) and FRET efficacy (right panel) measured in cells expressing various amounts of the GABA<sub>B</sub> receptor combinations illustrated in the top schemes: when both subunits carry a snap-tag (filled squares), when only GABA<sub>B1</sub> carries a snap-tag (grey circles), or when only GABA<sub>B2</sub> carries a snap-tag (open triangles). FRET intensity is plotted as a function of the amount of snap-tags at the cell surface deduced from the Bmax of [<sup>3</sup>H]-CGP54626. **(b)** FRET intensity as a function of the amount of ST-GABA<sub>B2</sub> expressed alone. **(c)** FRET between ST-GABA<sub>B2</sub> subunits as a function of the amount of transfected GABA<sub>B1</sub> plasmid. **(d)** GABA activation of the GABA<sub>B</sub> heteromer affects neither the FRET between GABA<sub>B2</sub> subunits

(GB1+ST-GB2), nor the FRET between GABA<sub>B1</sub> subunits (ST-GB1+GB2), nor the FRET between GABA<sub>B1</sub> and GABA<sub>B2</sub> subunits (ST-GB1+ST-GB2).

**Figure 5.** Functional correlate of the association between GABA<sub>B</sub> heterodimers **(a)** top: Scheme representing the various combinations of subunits co-expressed: ST-GABA<sub>B1</sub> (blue) with flag-GABA<sub>B2KKXX</sub> (red, the KKXX motif being the intracellular retention sequence added after the coiled coil domain), with (right) or without (left) the HA-GB1-HD, corresponding to the GB1 subunit deleted of both its extracellular and intracellular domains. Bottom: TR-FRET intensities measured between two ST-GABA<sub>B1</sub> labeled with BG-K and BG-d2 (left (1)), between ST-GABA<sub>B1</sub> labeled with BG-K and HA-GB1-HD labeled with d2-conjugated anti-HA antibodies (middle (2)), and between ST-GABA<sub>B1</sub> labeled with BG-K and flag-GABA<sub>B2KKXX</sub> labeled with d2-conjugated anti-flag antibodies (right (3)), in the absence (white columns) and in the presence (grey columns) of HA-GB1-HD. **b)** Ca<sup>2+</sup> signals generated in cells expressing ST-GABA<sub>B1</sub> and flag-GABA<sub>B2KKXX</sub> together (filled squares), or in the presence of over-expressed HA-GB1-HD (open squares), or in the presence of over-expressed CD4 (filled circles). Data are means ± sem of triplicate determinations from a typical experiment.

## Supplementary method:

**Determination of the  $R_0$  for the FRET between BG-K and BG-d2.**  $R_0$ , the Förster radius, is defined as the distance at which the FRET process is 50% efficient.  $R_0$  between the europium cryptate PBP and d2 was determined to be 65.4 Å using the following formula:

$$R_0 = \left( J \times 10^{-3} \times k^2 \times n^{-4} \times Q_D \right)^{1/6} \times 9730$$

Previous to  $R_0$  determination,  $J$ , the Förster integral overlap, was determined to be  $8.7 \times 10^{-10} \text{ cm}^6 \cdot \text{M}^{-1}$  using the following formula:

$$J = \frac{\int F_D(\lambda) \epsilon_A(\lambda) \lambda^4 d\lambda}{\int F_D(\lambda) d(\lambda)}$$

where  $F_D(\lambda)$ , the relative fluorescence intensity of the donor at wavelength  $\lambda$  and  $\epsilon_A(\lambda)$ , the molar extinction coefficient of the acceptor at wavelength  $\lambda$  were determined between 570nm and 720nm. To determine  $F_D$  at each wavelength  $\lambda$ , the fluorescence emission spectrum of the europium cryptate PBP, previously diluted at  $5 \mu\text{M}$  in a phosphate buffer pH=7 containing 0.1% BSA, was acquired on a LS50B spectrofluorimeter (Perkin Elmer).  $F_D(\lambda)$  was calculated by dividing the fluorescence intensity obtained at each wavelength by the value of the total fluorescence emitted between 570nm and 720nm.  $\epsilon_A(\lambda)$  was obtained for each wavelength  $\lambda$  using the following formula:

$$\epsilon_A = \frac{O.D.(\lambda)}{O.D.(649\text{nm})} \times 239,000$$

Where the  $\epsilon_A$  value at 649nm was considered to be equal to  $239,000 \text{ M}^{-1} \cdot \text{cm}^{-1}$ . The optical density at each wavelength,  $O.D.(\lambda)$ , was obtained through the acquisition of an absorption spectrum of d2 previously diluted at  $6 \mu\text{M}$  in a phosphate buffer pH=7 containing 0.1% BSA. Spectrum acquisition was done on a DU800 spectrophotometer (Beckman Coulter).

$Q_D$ , the luminescence quantum yield of the europium in the absence of the acceptor d2, was previously determined to be 0.48 (unpublished data).

The other parameters needed to perform a  $R_0$  determination were determined according to Selvin and Hearst.  $k^2$ , the dipole orientation factor was assumed to be 2/3,  $n$ , the medium refractive index, was fixed at 1.33.

Ref.: Selvin, P.R. & Hearst, J.E. (1994) *Proc Natl Acad Sci U S A* **91**, 10024-10028.

## Legends to supplementary figures

### Supp. Figure A:

(a) Light emission intensity of BG-K at 620 nm, 50 to 2500 $\mu$ s after laser excitation at 337nm.  
(b) Emission spectra of BG-K (black line) and BG-d2 (grey line) after excitation at 337nm and 640nm, respectively.

### Supp. Figure B:

Functional characterization of ST-GABA<sub>B1</sub> and ST-GABA<sub>B2</sub>. (a) Anti-HA (white columns) and anti-flag (black columns) ELISA performed on intact cells expressing the indicating subunits. (b) Saturation binding experiments using [<sup>3</sup>H]-CGP54626 on intact cells expressing either GABA<sub>B1</sub> and GABA<sub>B2</sub> (black squares) or ST-GABA<sub>B1</sub> and GABA<sub>B2</sub> (open squares). (c) Ca<sup>2+</sup> signals generated by increasing concentrations of GABA in cells expressing ST-GABA<sub>B1</sub> and GABA<sub>B2</sub> (grey triangles), GABA<sub>B1</sub> and ST-GABA<sub>B2</sub> (open circles) or GABA<sub>B1</sub> and GABA<sub>B2</sub> (black squares). Data are means  $\pm$  s.e.m. of triplicate determinations from typical experiments.

### Supp. Figure C:

Scheme describing the synthesis of BG-K (5) used in this study.

### Supp. Figure D:

Anti-HA (white columns) and anti-flag (black columns) ELISA performed on intact cells expressing the indicating subunits.

### Supp. Figure E:

FRET signal measured as the  $\Delta$ 665 signal in cells expressing various amounts of HA-ST-GABA<sub>B1a</sub> and ST-GABA<sub>B2</sub> (black squares) or HA-ST-GABA<sub>B1b</sub> and ST-GABA<sub>B2</sub> (open squares). Cell surface amount of the recombinant receptors was determined using [<sup>3</sup>H]-CGP54626 saturation binding experiments. Data are means  $\pm$  s.e.m. of triplicate determination from a typical experiment.

### Supp. Figure F:

Schematic representation of some possible arrangements of a dimer of GABA<sub>B</sub> heterodimers, and the deduced FRET efficacy determined using the Förster equation  $E=R_0^6/(d^6+R_0^6)$  where  $R_0$

is the distance between the fluorophores giving rise to 50% FRET efficacy, and determined to be 65Å, and d is the distance between the fluorophores, assuming the distance between the fluorophores is similar to the distance between the N-terminus of the subunits. According to the presence of the snap-tag fusion, these distances are  $\pm 20\text{\AA}$ .

**Supp. Figure G:**

Percent of surface expression determined as the ratio between the ELISA signals measured on intact cells over that measured after cell permeabilization of the indicated subunits. Anti-flag (top) and anti-HA (bottom) ELISA. Data are means  $\pm$  s.e.m. of triplicate determinations from a typical experiment.

**Supp. Figure H:**

BRET signals was measured in cells expressing a constant amount of GABA<sub>B1</sub>-Rluc, and i) increasing amounts of GABA<sub>B2</sub>-YFP (filled squares), ii) increasing amounts of GABA<sub>B1</sub>-YFP (and an excess of GABA<sub>B2</sub>) (open circles), and iii) increasing amounts of the thrombin receptor PAR1-YFP (and an excess of GABA<sub>B2</sub>) (open triangles). Data are means  $\pm$  s.e.m. of triplicate determinations and data from 3 independent experiments were pooled.

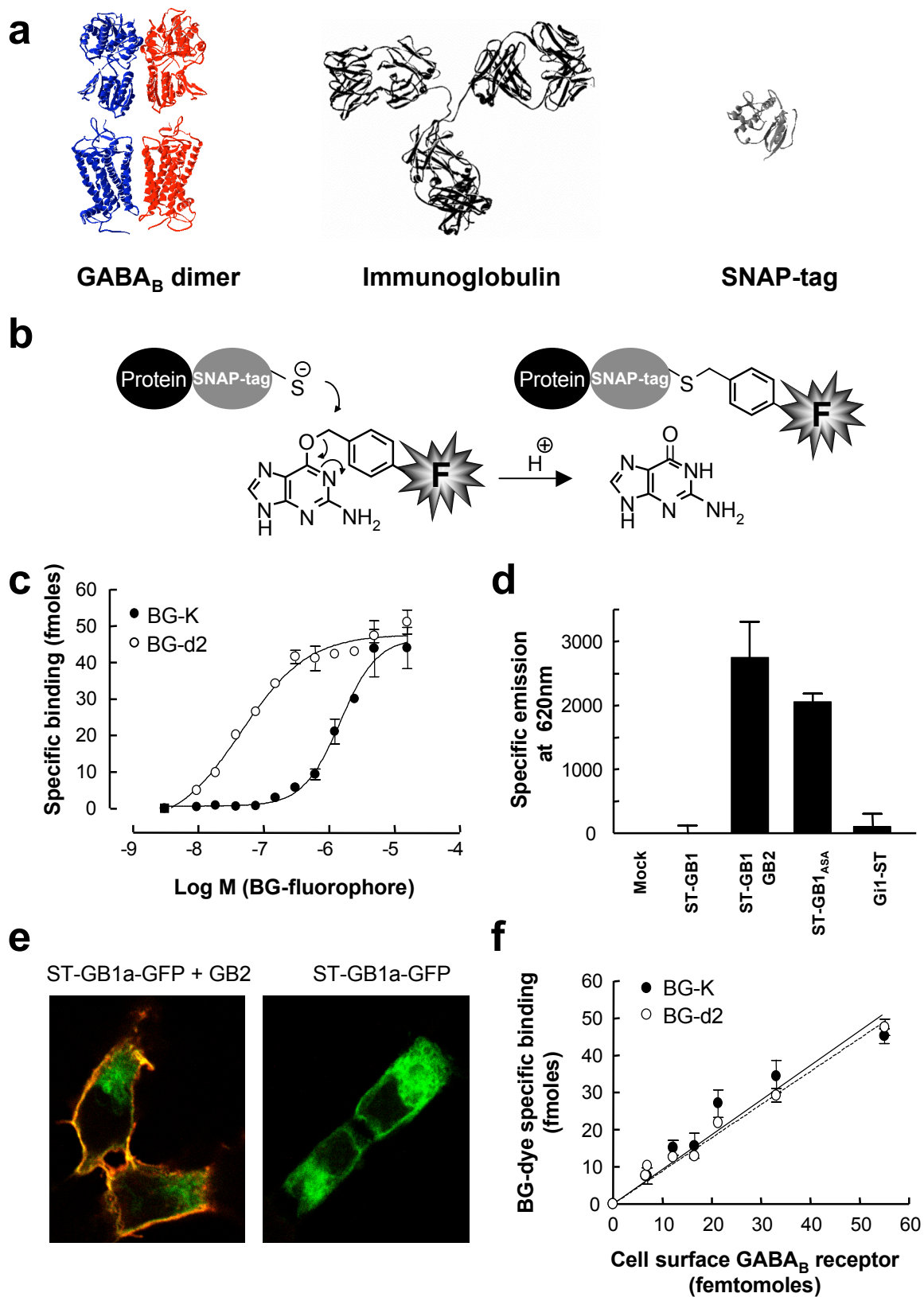


Figure 1

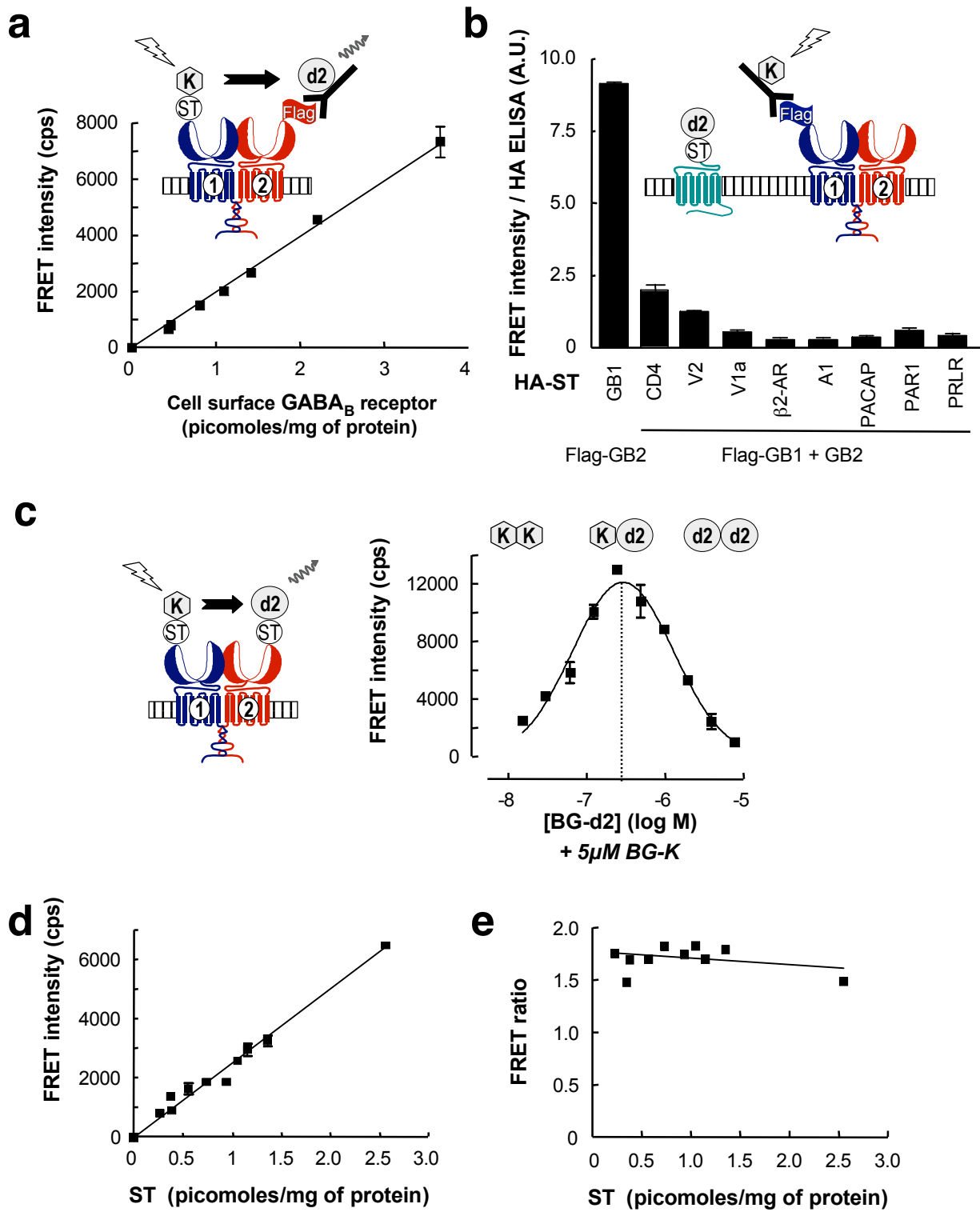
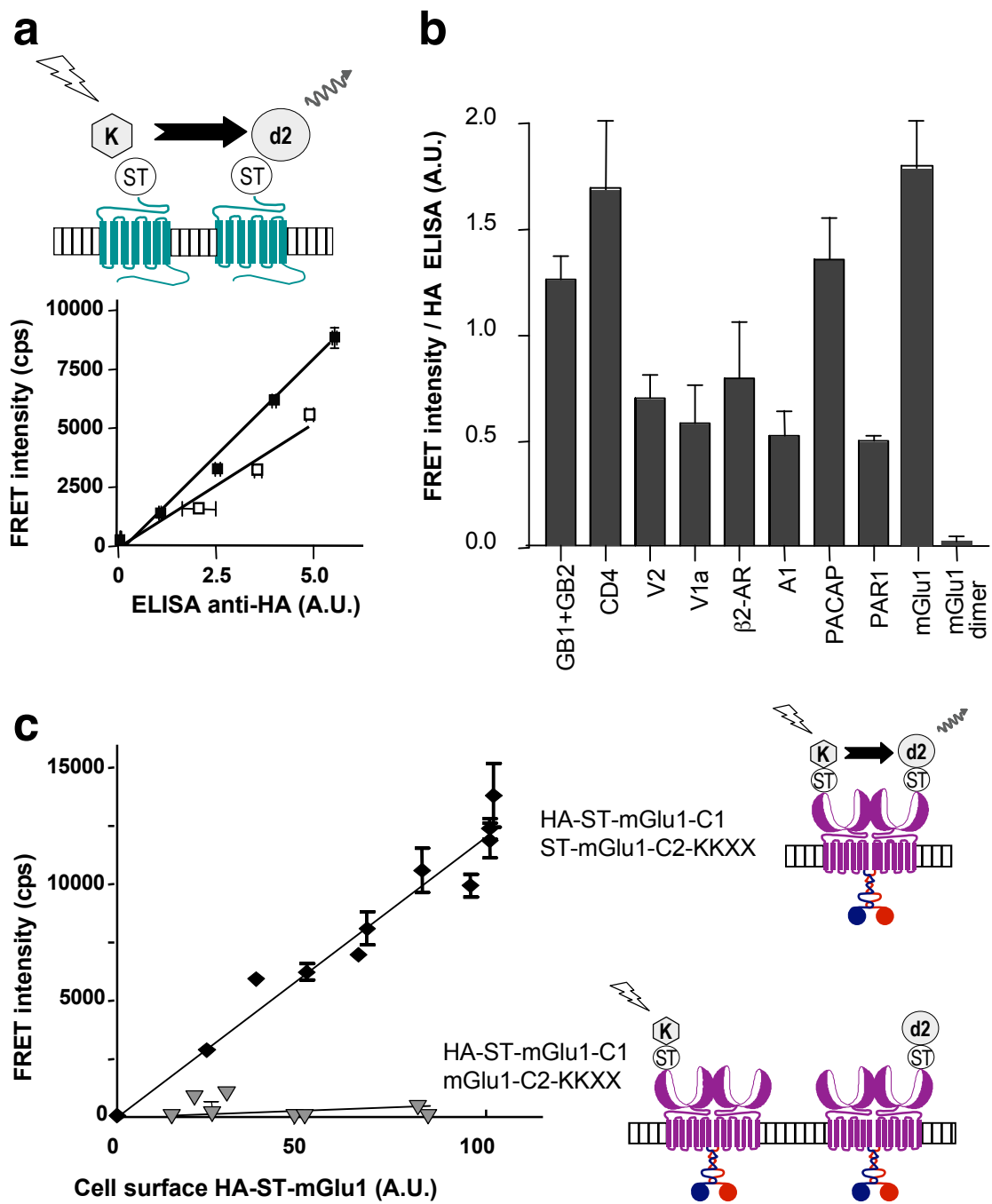
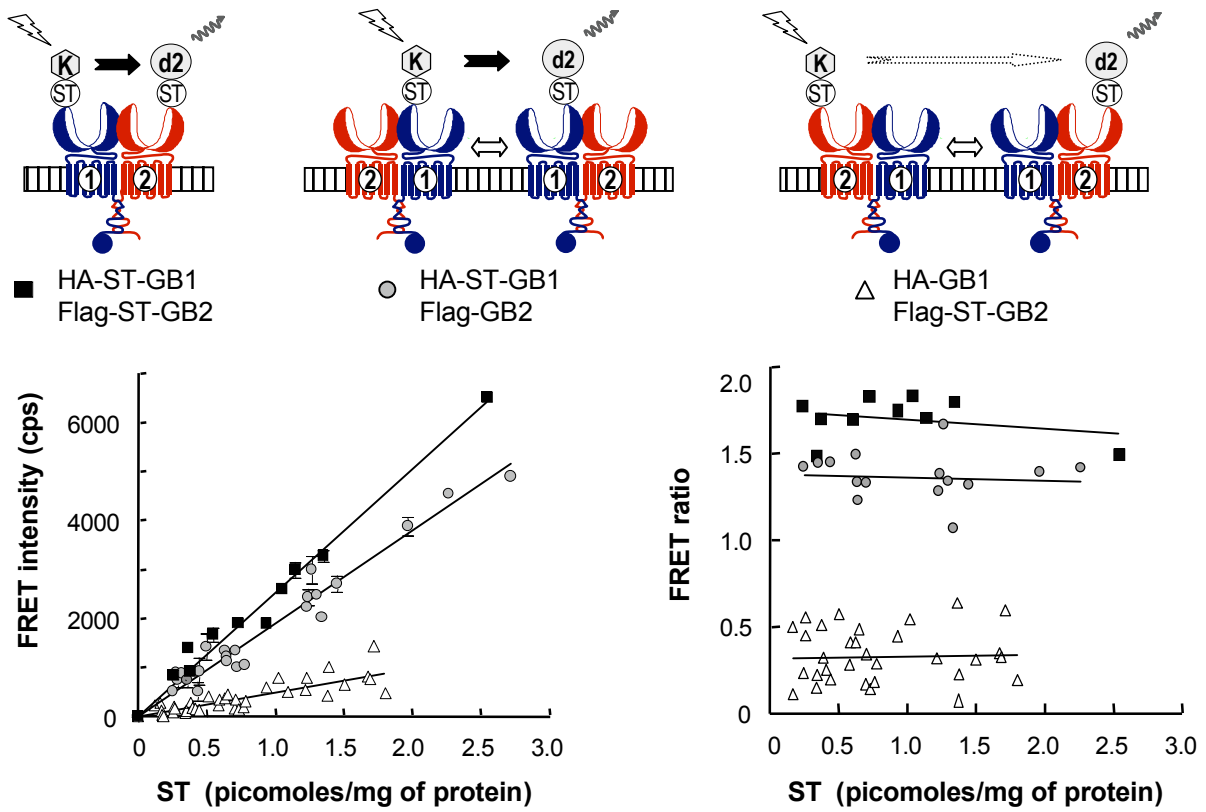
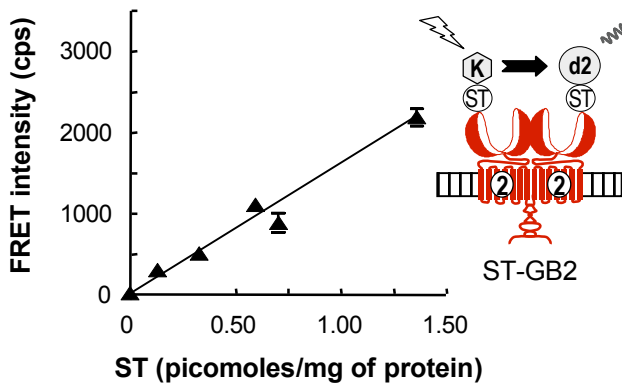
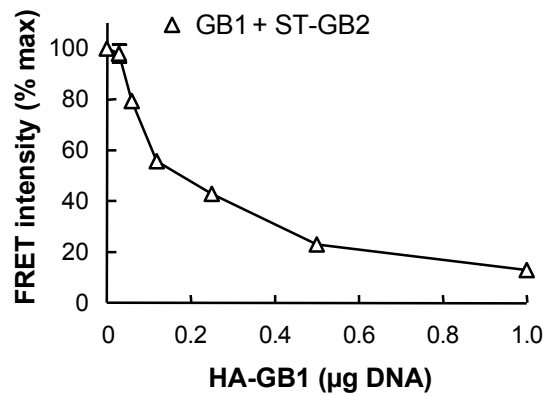
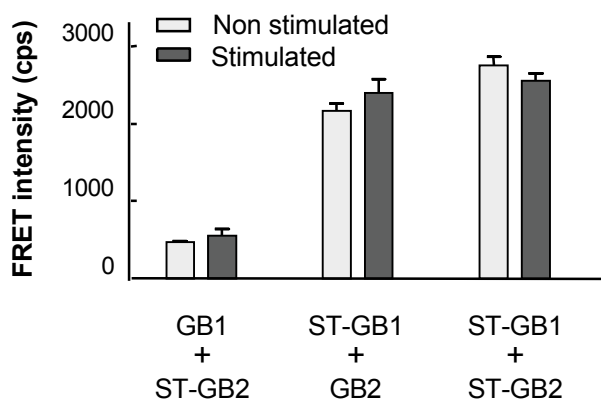
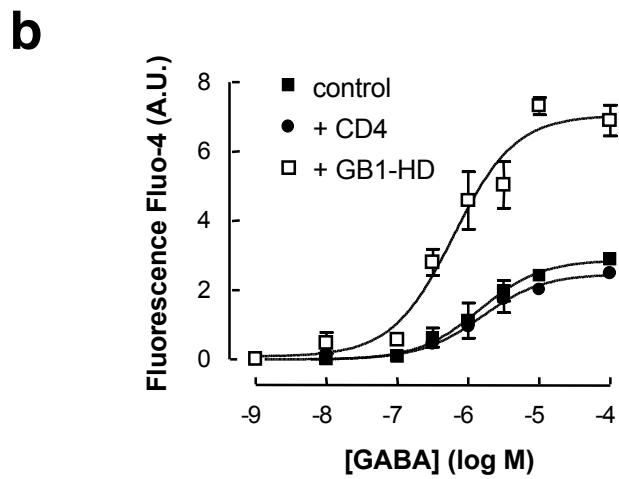
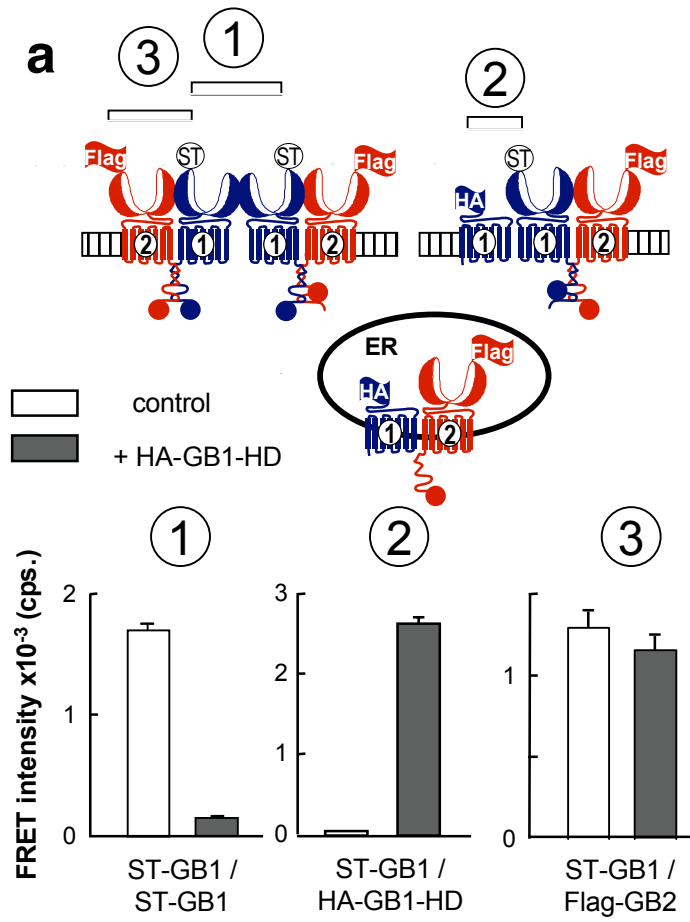


Figure 2

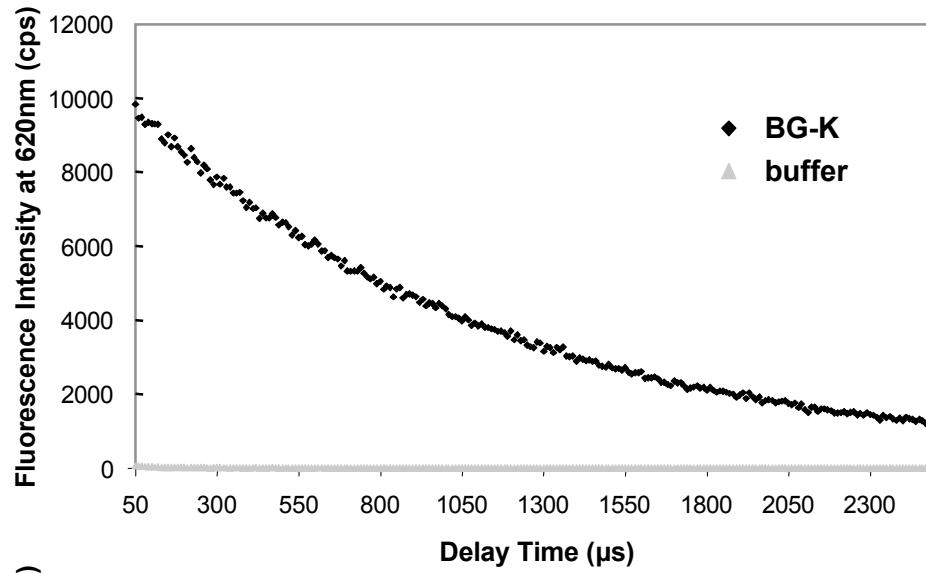
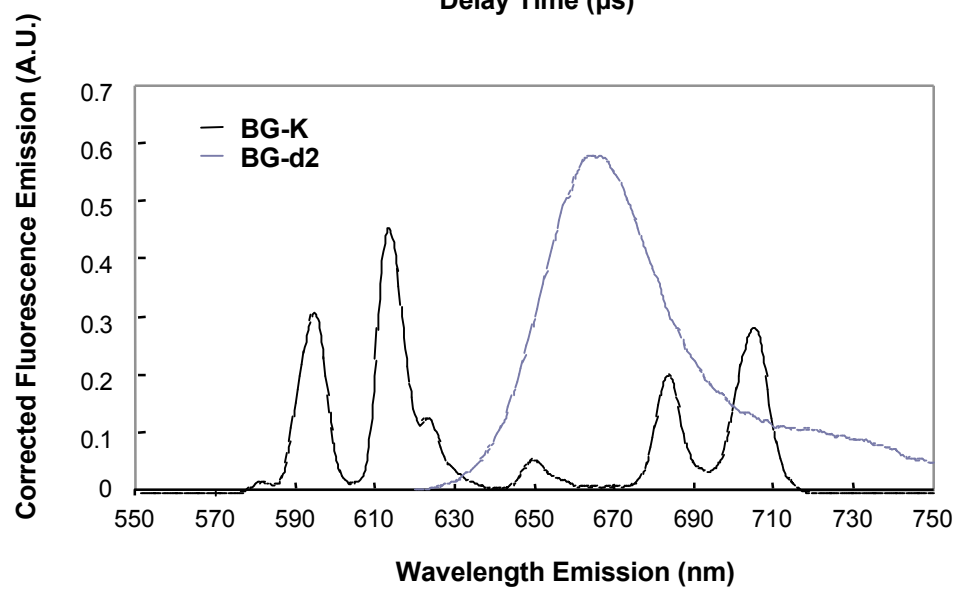


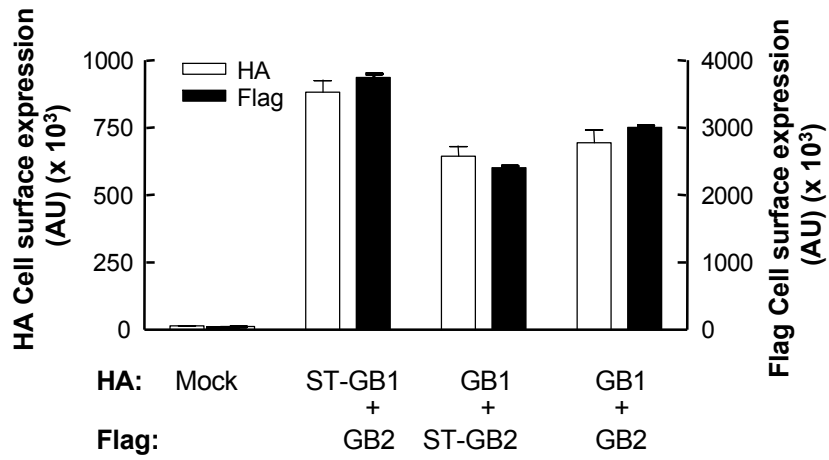
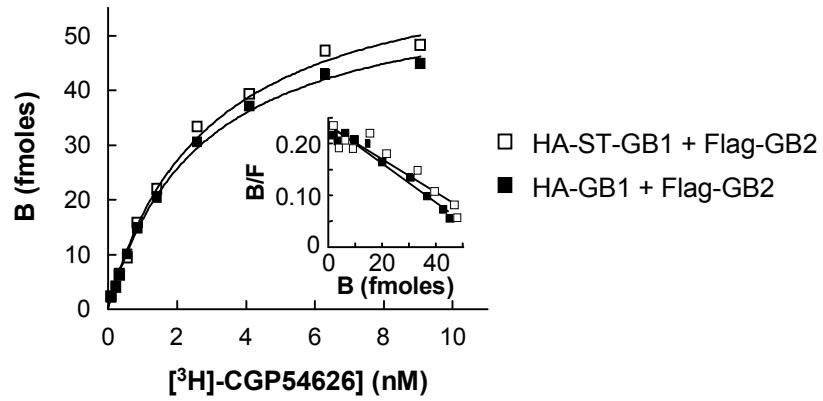
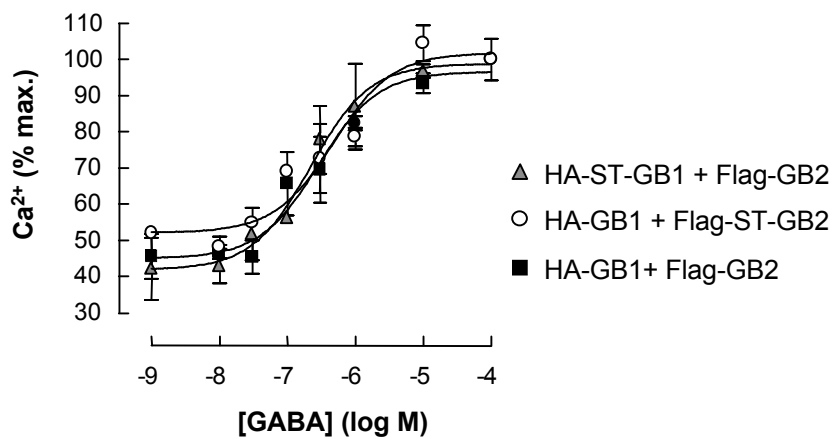
**Figure 3**

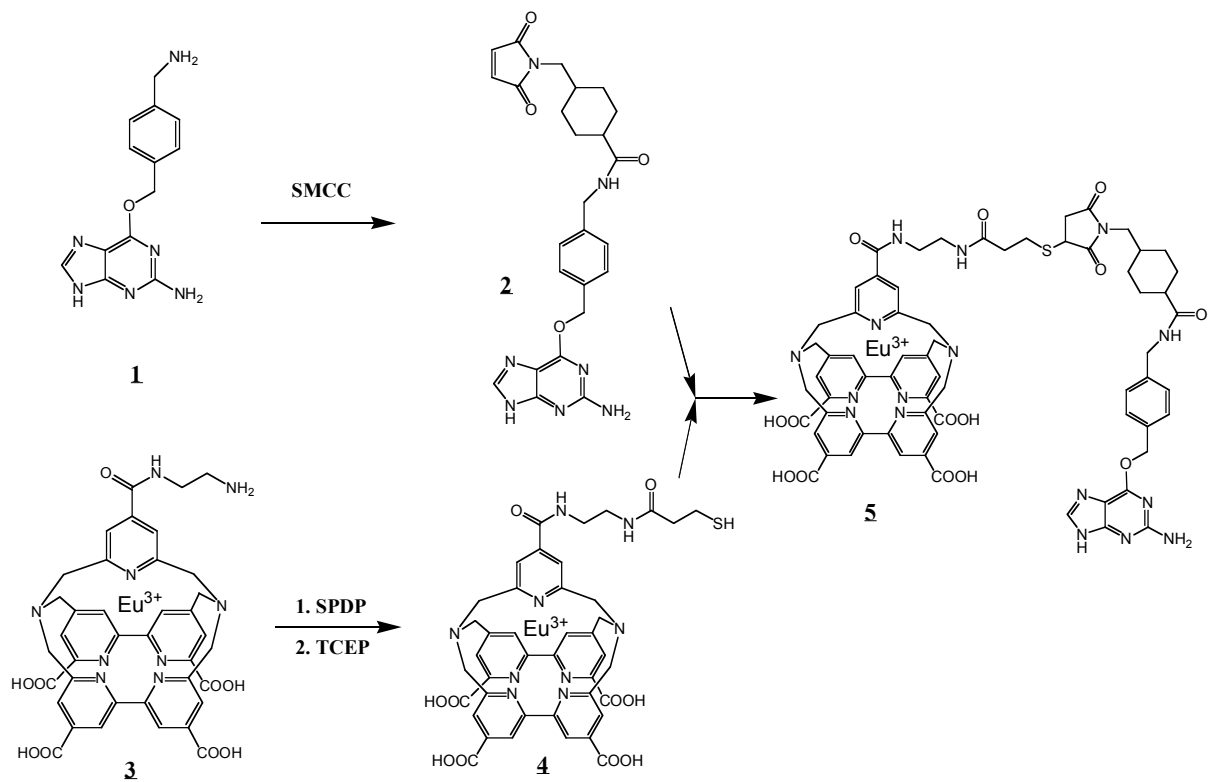
**a****b****c****d****Figure 4**



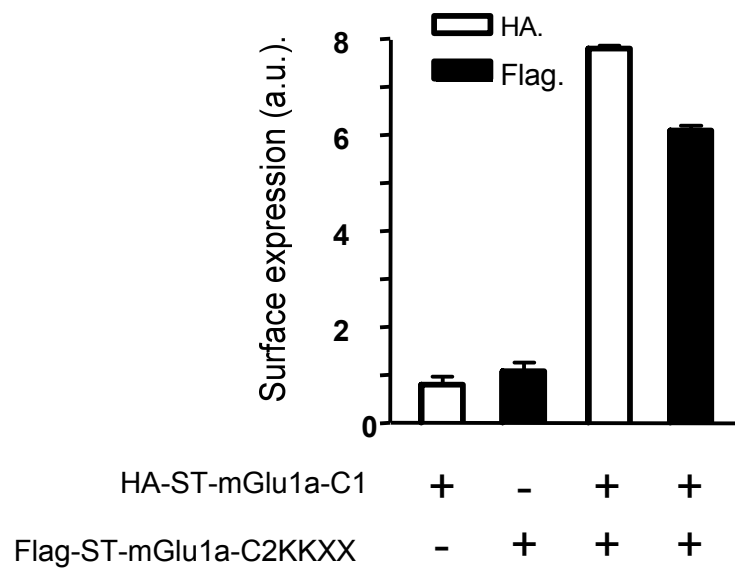
**Figure 5**

**a****b****Supp Fig. A**

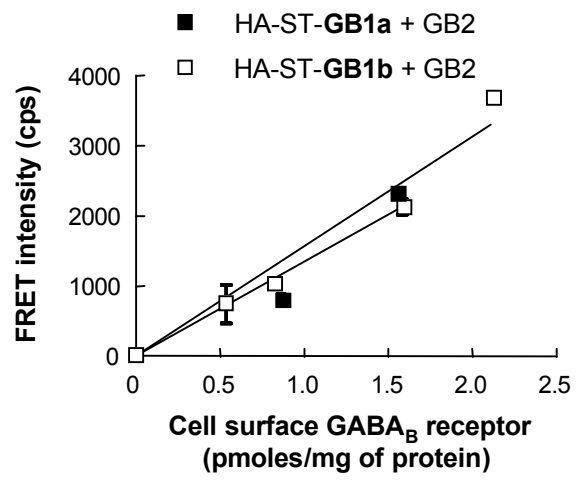
**a****b****c****Supp Fig. B**



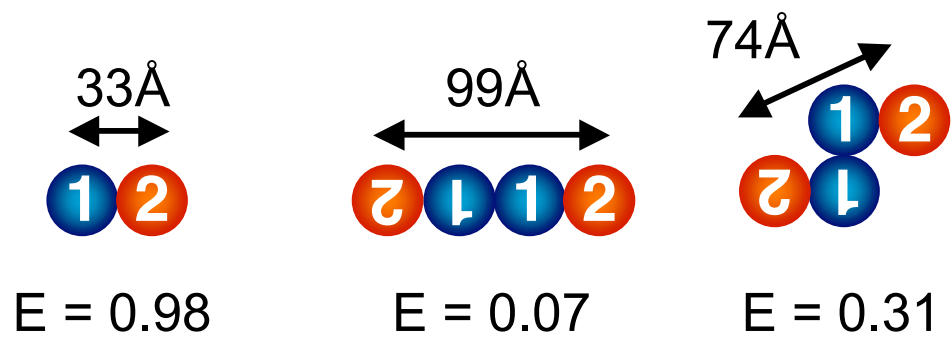
**Supp Fig. C**



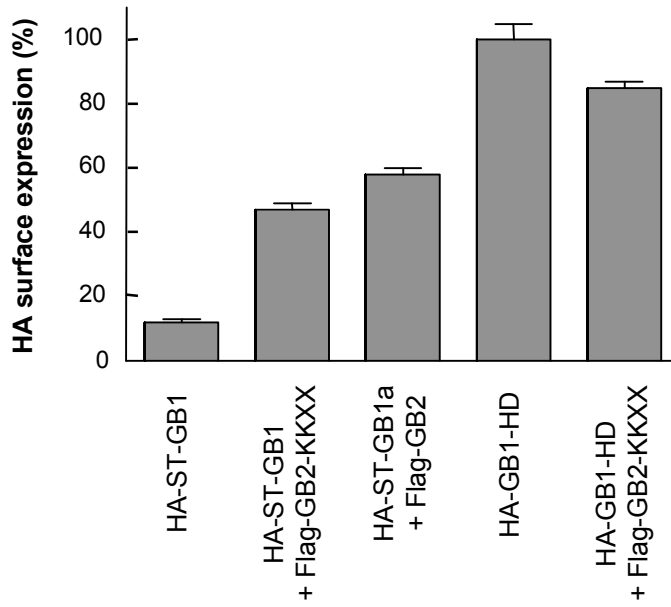
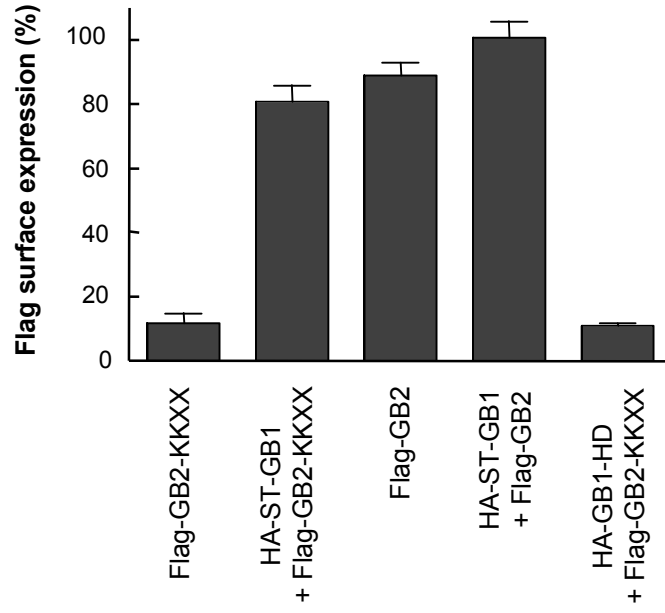
**Supp Fig. D**



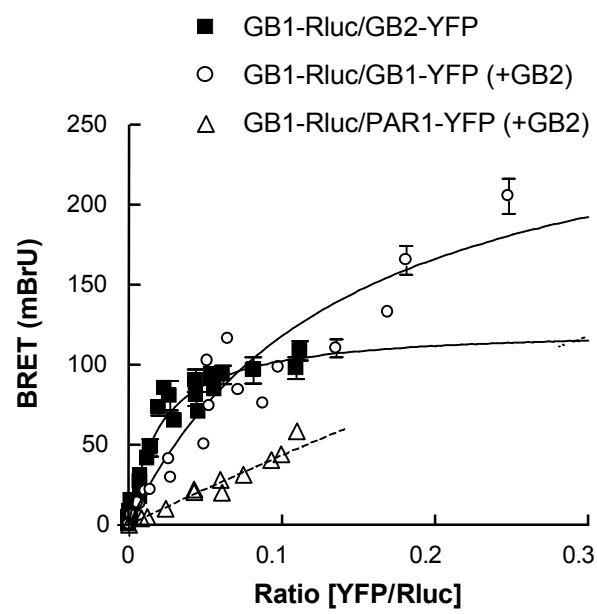
**Supp Fig. E**



Supp Fig. F



**Supp Fig. G**



Supp Fig. H